

## Investigation of Anodic Behavior of Nickel in H<sub>2</sub>SO<sub>4</sub> Solutions Using Galvanostatic Polarization Technique. II. Initiation and Inhibition of Pitting Corrosion by Some Inorganic Passivators

S. Abd El Wanees<sup>1,2,\*</sup>, Arej S. Al-Gorair<sup>3</sup>, H. Hawsawi<sup>4</sup>, S. S. Elyan<sup>5</sup>, M. Abdallah<sup>6,7</sup>

<sup>1</sup> Faculty College of Umluj, Umluj, Tabuk University, Tabuk, Saudi Arabia.

<sup>2</sup> Chemistry Department, Faculty of Science, Zagazig University, Zagazig, Egypt

<sup>3</sup> Chemistry Department, College of Science, Princess Nourah bint Abdulrahman University, Riyadh, Saudi Arabia

<sup>4</sup> University College of Alwajh, Alwajh, Tabuk University, Tabuk, Saudi Arabia

<sup>5</sup> Chemistry Department, Faculty of Pharmacy, Badr University in Cairo (BUC), Badr City, Egypt

<sup>6</sup> Chemistry Department, Faculty of Science, Umm Al-Qura University, Makkah Al Mukaramha, Saudi Arabia

<sup>7</sup> Chemistry Department, Faculty of Science, Banha University, Banha, Egypt

\*E- mail: [s\\_wanees@yahoo.com](mailto:s_wanees@yahoo.com)

Received: 11 January 2021 / Accepted: 1 March 2021 / Published: 31 March 2021

The anodic polarization of nickel in dilute sulfuric acid media was investigated in the absence and presence of ClO<sub>4</sub><sup>-</sup> ions, at a constant current density. The anodic polarized curve is characterized by a sudden jump in potential owing to the decay of H-over voltage, followed by two oxidation arrests, passive and O<sub>2</sub> evolution regions. The presence of ClO<sub>4</sub><sup>-</sup> ions distorts the polarized curve owing to the damage in the passive film with the initiation of localized pitting corrosion, at pitting potential,  $E_{pit}$ .  $E_{pit}$  displaces into active direction with rising amounts of the ClO<sub>4</sub><sup>-</sup> ions. The presence of various concentrations of Na<sub>2</sub>HPO<sub>4</sub>, Na<sub>2</sub>MoO<sub>4</sub> and Na<sub>2</sub>CrO<sub>4</sub> shift the  $E_{pit}$  into more positive values, confirming the suppression of pitting corrosion. The anions of these salts displace the  $E_{pit}$  into the more noble direction due to a competition with the ClO<sub>4</sub><sup>-</sup> ions. The inhibition effect towards the pitting corrosion of Ni follows the sequence Na<sub>2</sub>HPO<sub>4</sub> > Na<sub>2</sub>MoO<sub>4</sub> > Na<sub>2</sub>CrO<sub>4</sub>. Thermodynamics activation energies required for the destruction of the passive film,  $E_a$ , are estimated and explained in the absence and presence of the different anions.

**Keywords:** Nickel; Galvanostatic; Pitting Corrosion; Inhibition; Oxide film; Passivity.

### 1. INTRODUCTION

Ni and its alloys indicate high corrosion immovability in various electrolytic media due to the presence of a stationary passive oxide layer on its external surface [1-7]. The quality of consistence of

such film relies on considerable factors within which the strength of the solution, pH, existence of corrosive or inhibitive ions, and the solution temperature [8-10].

The resistance of Ni to the corrosion process is attributed to the presence of a preventative oxide, a hydrated oxide film[11], and/or to a chemical adsorbed O-layer on its surface[12]. The passivity of nickel in aqueous acidic solutions could be attributed to the rising in the conductivity of the formed oxide film[13]. Previous investigations about the potentiokinetic polarization for Ni indicated considerable conflicts [14-16]. These were ascribed to nature and the impurities in each of the investigated metals [14] and electrolytes, as well as the variations in the experimental procedures [15].

Localized pitting corrosion initiates when the passive film is emaciated at a definite weak point on the metal surface, performing quick corrosion for the protected metal [17-21]. Many investigators indicated that a localized type of attack takes place when the passive metal is exposed to electrolytic solutions containing halide anions [10,17-22]. Also, such a type of attack may also occur in the presence of  $\text{ClO}_3^-$  and  $\text{ClO}_4^-$  ions[23-27]. Breakdown of passivity in the presence of  $\text{ClO}_4^-$  ions is usually restricted to certain potential ranges [25].

The current paper is to highlight the effect of  $\text{ClO}_4^-$  ions in the initiation and propagation of localized pitting corrosion on nickel in 0.01 M  $\text{H}_2\text{SO}_4$  solutions using the anodic galvanostatic polarization method. Trails are done to inhibit such a type of attack employing  $\text{Na}_2\text{HPO}_4$ ,  $\text{Na}_2\text{MoO}_4$  and  $\text{Na}_2\text{CrO}_4$ . The influence of temperature on the initiation and inhibition of pitting corrosion are investigated. The activation energies required for oxide film destruction and initiation of pitting corrosion are calculated and explained in the absence and presence of such passivators. Surface examination for some corroded Ni samples is investigated in the absence and presence of corrosive and inhibitive anions.

## 2. MATERIALS AND METHODS

### 2.1. Materials

The working electrode employed in this investigation was a pure nickel metal was described in the recent literature of this study [4]. The electrical connection of the Ni electrode was carried by using a pure thick copper wire with 2 mm diameter. The rod was fixed into a borosilicate glass pipe using an epoxy resin leaving 0.97 cm<sup>2</sup> of a naked free cross-sectional surface area. Prior to running the experiment, the surface area of the Ni electrode was cleaned mechanically by abrading with various grades of fine polished papers. Then, the electrode was cleaned by rinsing with acetone followed by bi-distilled water and the test solution before inundation in the investigated solution.

The required solutions were prepared from A.R.  $\text{H}_2\text{SO}_4$  and  $\text{NaClO}_4$  (Fluka) and a bi-distilled water. Various amounts of  $\text{Na}_2\text{HPO}_4$ ,  $\text{Na}_2\text{MoO}_4$  and  $\text{Na}_2\text{CrO}_4$  are added to 0.01 M  $\text{H}_2\text{SO}_4$  containing 0.01 M  $\text{NaClO}_4$ . Experiments were done at 25°C, except otherwise carried at various temperatures. The scanning electron microscope, JEOL TM, JSM- T100 (Japan), is used to examine the surface of some

corroded Ni surfaces in 0.01 M H<sub>2</sub>SO<sub>4</sub> + 0.01 M NaClO<sub>4</sub> in the absence and presence of 0.01 M Na<sub>2</sub>MoO<sub>4</sub>.

## 2.2. The Electrolytic cell

The used electrolytic cell was described early [28-31]. Three kinds of electrodes are employed (platinum wire as a counter electrode, nickel as a working electrode, and a saturated calomel electrode, SCE, as a reference electrode). An ultra-thermostat Polyscience-type (USA) was used for adjusting the reaction temperature. Each test was done with a newly prepared electrode and a neoteric solution. The potential-time curves at a constant applied current were plotted on a recorder unit, Cole Parmer Instruments (USA).

## 3. RESULTS AND DISCUSSION

### 3.1. The effect of ClO<sub>4</sub><sup>-</sup> ions concentration

Figs 1 depicts the anodic polarized curves of nickel in 0.01M H<sub>2</sub>SO<sub>4</sub> solutions without and with the additions of various amounts of ClO<sub>4</sub><sup>-</sup> ions, at 1.0 mA/cm<sup>2</sup> and 25°C.

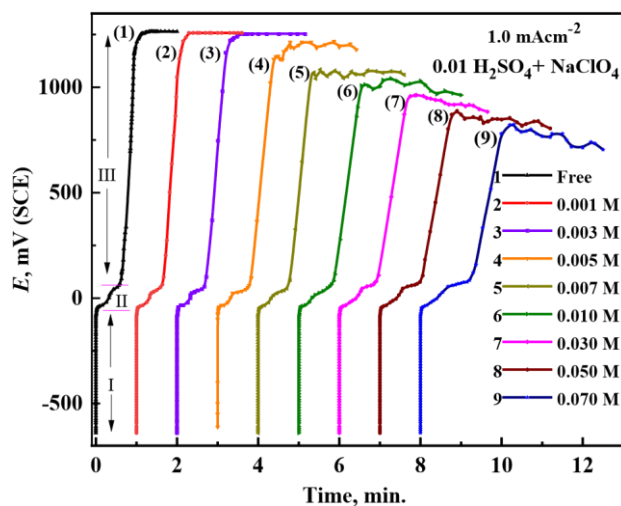


**Figure 1.** Galvanostatic anodic polarization curves of Ni, at 1.0 mA/cm<sup>2</sup>, in 0.01 M H<sub>2</sub>SO<sub>4</sub> containing different concentrations of NaClO<sub>4</sub>, at 1.0 mA/cm<sup>2</sup> and 25°C.

The curves are distinguished by a swift jump of the potential (region I) confirming the decay of hydrogen over-potential on the nickel surface accompanied by charging of the electrical double layer at the metal/solution interface [4, 32,33]. Prior to the decay step (region I), the potential of the nickel electrode modifies slowly with reaction time to give two distinct dissolution arrests, **a** and **b** (zone II) followed by an oblique rise in the potential-time curve (zone III). However, the ClO<sub>4</sub><sup>-</sup> ions free

polarized curve indicated different characteristic regions assuring different oxidation stages followed by passive film formation and O<sub>2</sub> evolution regions. The oxidation processes indicated by the arrests **a** and **b** generate monovalent and divalent nickel cations which are easily turned to NiO by the effect of water[4, 34-36]:



The hop in the *E* towards the noble values, after the active oxidation process, could be imputed to the precipitation of the nickel oxides on the anode surface, producing the passive oxide film [4]. However, It is clear from the curves of Fig 1 that the presence of different amounts of ClO<sub>4</sub><sup>-</sup> ions could impact the shape of the anodic polarized curves. Few additions of ClO<sub>4</sub><sup>-</sup> ions (< 0.003 M) do not influence the general shape of the polarized curve gained in ClO<sub>4</sub><sup>-</sup> ions-free electrolyte. Relatively higher additions of ClO<sub>4</sub><sup>-</sup> ions (> 0.003 M) distort the anodic polarized curves owing to the damage of the passive oxide film with the initiation of localized pitting corrosion at localized active cells[10, 32]. The initiation of localized pitting attack on the passive nickel oxide film can take place at a specific additions of the ClO<sub>4</sub><sup>-</sup> ions and above a critical value [32, 37].

Furthermore, Fig 1 depicts that the presence of 0.003M ClO<sub>4</sub><sup>-</sup> ions produces little potential fluctuations during the O<sub>2</sub> evolution-region. Such attitude elucidates that the ClO<sub>4</sub><sup>-</sup> ions interpose with the O<sub>2</sub> evolution [37]. The presence of fluctuations in this region may be referred to the truth that the passivation process happens jointly with the process of oxide film destruction. A state at which the rate of oxide film destruction is slightly exceeded that of oxide film formation, metastable pits are created [10]. The formed metastable pits are characterized by a very finite existence, that they passivated again and the potential, *E*, returned to the O-evolution region [37].

Is noteworthy to see that the fluctuations in potential are increased and shift to more negative directions as the amount of the added ClO<sub>4</sub><sup>-</sup> ions raises above the critical concentration[37]. These fluctuations in the potential may be referred to the destruction of passivity in the existence of ClO<sub>4</sub><sup>-</sup> ions and the passivation of the oxide film by the effect of the anodic current [37].

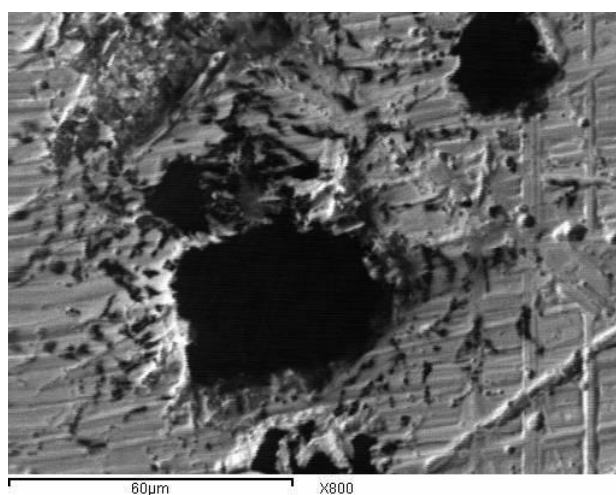


**Figure 2.** Scanning electron micrograph (SEM) of the anodically polarized Ni sample in 0.01 M H<sub>2</sub>SO<sub>4</sub> + 0.01M ClO<sub>4</sub><sup>-</sup> ions.

Higher concentrations of  $\text{ClO}_4^-$  ions  $\geq 0.007$  M cause variable changes in the general shape of the anodic polarized curve. The duration of the oxidation process, region II ( arrests **a** and **b**),  $\tau$ , increases whereas the rate of oxide film formation,  $\partial E/\partial t$ , reduces. Moreover, the breakdown of the passive film is attained at a definite potential,  $E_{\text{pit}}$ . At this potential,  $E_{\text{pit}}$ , fluctuations in the potential with time are noted without attaining the oxygen evolution, i.e., the damage of the passive oxide-film with the initiation of the localized pitting corrosion is observed [37, 38]. The pitting corrosion potential,  $E_{\text{pit}}$ , relocates into more active values, less positive, as the amounts of  $\text{ClO}_4^-$  ions are raised. Fig. 2 shows the scanning electron micrograph (SEM) of the anodic polarized Ni sample in 0.01 M  $\text{H}_2\text{SO}_4$  containing 0.01M  $\text{ClO}_4^-$  ions. The photograph indicates a number of irregularly distributed pits on the surface of the passive film. This confirms that the existence of  $\text{ClO}_4^-$  ions destruct the passive film with a generation of well-defined pits, distributed on the surface of the passive oxide film.

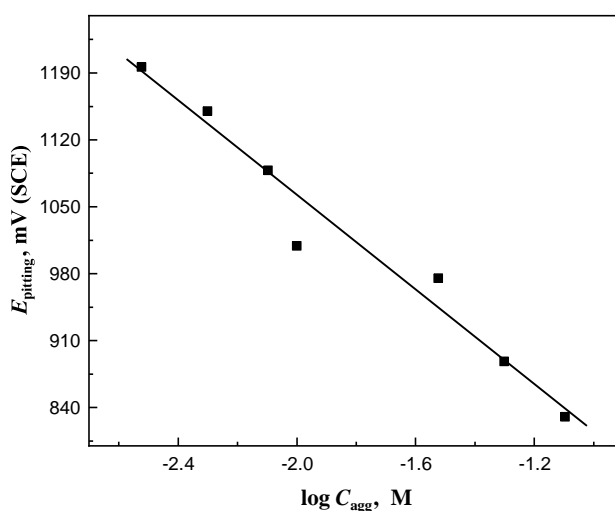


**Figure 3.** Variation of  $E_{\text{pitting}}$  with  $\log C_{\text{agg}}$  for Ni in 0.01 M  $\text{H}_2\text{SO}_4$ , at 25°C.

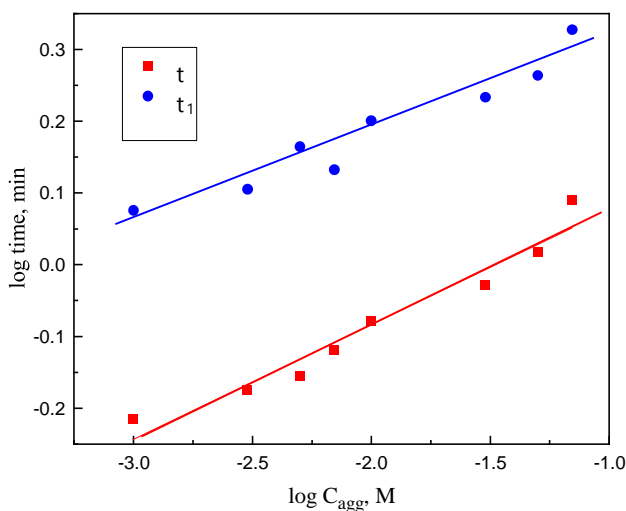


**Figure 4.** Variation of  $\log \tau$  and  $\log \tau_1$  against  $\log C_{\text{ClO}_4^-}$  for Ni in 0.01 M  $\text{H}_2\text{SO}_4$ , at 25°C.

The variation of the galvanostatic pitting corrosion potential,  $E_{\text{pit}}$ , with the logarithm of the added amount of  $\text{ClO}_4^-$  ions can be depicted in Fig 3. This figure illustrate the lowering of  $E_{\text{pit}}$  with the aggressive ions concentration according to the relation:

$$E_{\text{pit}} = \xi - \gamma \log C_{\text{ClO}_4^-} \quad (2)$$

where  $\xi$  and  $\gamma$  are constants that rely on the solution composition and the type of the aggressive anion. It is seen that the pitting potential,  $E_{\text{pit}}$ , decreases gradually with increasing the  $\text{ClO}_4^-$  ions concentration, due to the enhancement in the initiation of localized pits producing localized-type of attack, extremely pitting corrosion.

However, it noted from Fig 1 that the period of the active anodic oxidation indicated by the arrests **a** and **b** of region II,  $\tau$ , was also dependent on the concentration of  $\text{ClO}_4^-$  ions. Also, the exposure time of Ni electrode required for pit formation and the initiation of pitting corrosion is considered as the induction time,  $\tau_1$  [39]. The period of the arrests **a** and **b**,  $\tau$ , as well as, the induction time required for pitting corrosion,  $\tau_1$ , are elongated as the concentration of  $\text{ClO}_4^-$  ions is increased. A straight line relation is obtained when  $\log \tau(\tau_1)$  values are plotted against  $\log C_{\text{ClO}_4^-}$  (Fig 4) satisfying the following relation:

$$\log \tau = \alpha' + \beta' \log C_{\text{ClO}_4^-} \quad (3)$$

where  $\alpha'$  and  $\beta'$  are constants that rely on the solution composition and its type.

Fig 5 depicts the divergence in the rate of oxide-film formation,  $(\partial E/\partial t)_i$ , with the  $\log C$  of the added  $\text{ClO}_4^-$  ions.

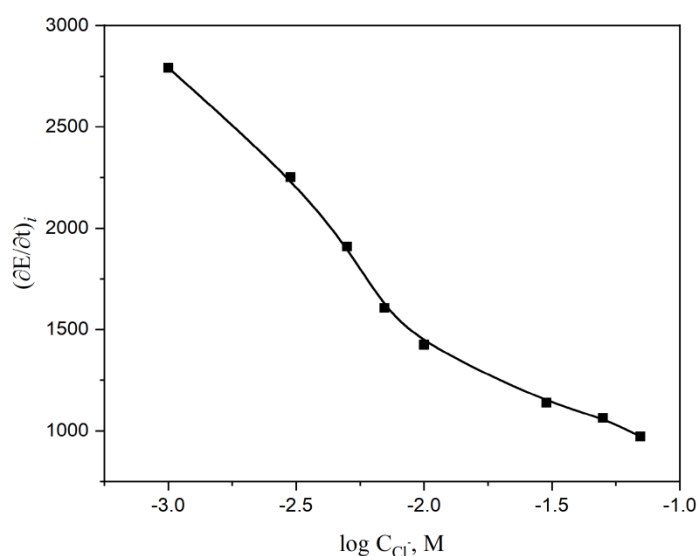


**Figure 5.** Variation of the rate of oxide-film formation,  $(\partial E/\partial t)_i$ , with the  $\log C_{\text{ClO}_4^-}$  ions for Ni in 0.01 M  $\text{H}_2\text{SO}_4$ , at 25°C.

This figure depicts the reduction in the  $\partial E/\partial t$  values with the added  $\text{ClO}_4^-$  amounts, according to the segmented S-shaped curve. This attitude could confirm the existence of an adsorption process for  $\text{ClO}_4^-$  anions on the passive oxide-film before the permeation of this film and initiation of the localized pitting corrosion[40].

From another point of opinion, Pagitsas et al. have confirmed that the provenance of localized pitting corrosion generated by  $\text{ClO}_4^-$  ions is due to the penetration of this film by the formed  $\text{Cl}^-$  ions[23,24]. The chloride ions are formed via the reduction of perchlorate ions by  $\text{Ni}^{2+}$  following the overall equation [23, 24]:



Thus, increasing the addition of  $\text{ClO}_4^-$  ions boosts the oxide destruction since more chlorides are produced and adsorbed on the passive metal surface. The initiation of pits is owing to the ability of  $\text{ClO}_4^-$  and/or  $\text{Cl}^-$  ions to impede oxide film formation causing further metal dissolution [41] and more  $\text{Cl}^-$  ions migrated into the breakdown metal area.

### 3.2. The influence of additions of inorganic passivators as inhibitors.

The effect of the addition of  $\text{Na}_2\text{HPO}_4$ ,  $\text{Na}_2\text{MoO}_4$  and  $\text{Na}_2\text{CrO}_4$  on the anodic polarization curve of nickel in 0.01 M  $\text{H}_2\text{SO}_4$  containing 0.01 M  $\text{ClO}_4^-$  ions was studied. Fig 6 depicts the galvanostatic anodic polarized curves for nickel in 0.01 M  $\text{H}_2\text{SO}_4$  containing 0.01 M  $\text{ClO}_4^-$  ions in the existence of various additions of  $\text{Na}_2\text{MoO}_4$ , at 1 mA/cm<sup>2</sup> and 25°C. Comparable data are gained with the additions of  $\text{Na}_2\text{HPO}_4$  and  $\text{Na}_2\text{CrO}_4$  (curves not shown). Fig 6 and the likes indicate that the addition of the different inhibitors reduces the period of the oxidation process, increase the rate of oxide film formation,  $(\partial E/\partial t)_i$ , and shift the pitting potential,  $E_{\text{pit}}$ , into the noble direction to an extent that depends on the amount and the kind of the used salt,  $C_{\text{inh}}$ .

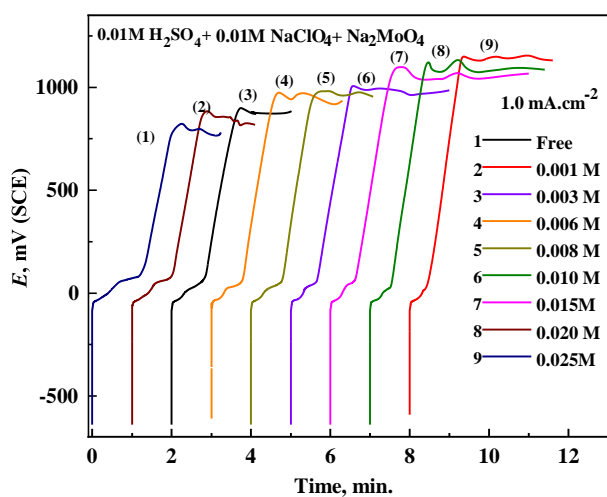


**Figure 6.** Galvanostatic anodic polarization curves of Ni in 0.01 M  $\text{H}_2\text{SO}_4$  containing 0.01 M  $\text{NaClO}_4$  and different additions of  $\text{Na}_2\text{MoO}_4$ , at 1.0 mA/cm<sup>2</sup> and 25°C.

Fig 7 explores the reliance of the  $(\partial E/\partial t)_i$  on the amount of the added salt,  $C_{inh}$ . S-shaped curves are gained when  $(\partial E/\partial t)_i$  values are plotted against the  $\log C_{inh}$ , confirming the existence of an adsorption process competing with the  $ClO_4^-$  ions [42].

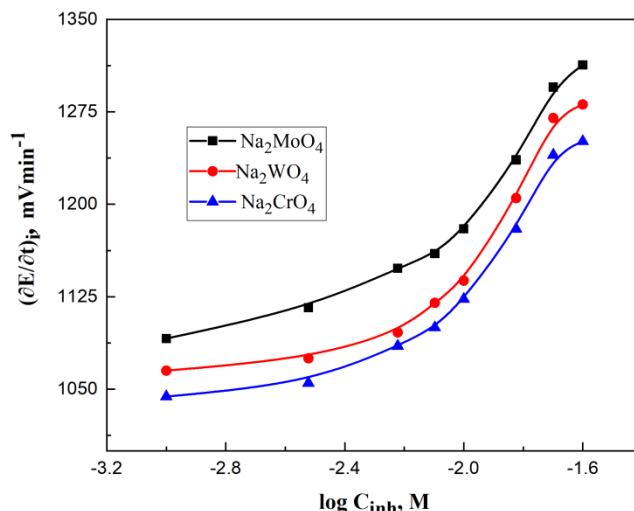


**Figure 7.** Variation of  $(\partial E/\partial t)_i$  with the concentration of the inhibitor,  $C_{inh}$  for Ni in 0.01M  $H_2SO_4$  containing 0.01 M  $NaClO_4$ , at 25°C.

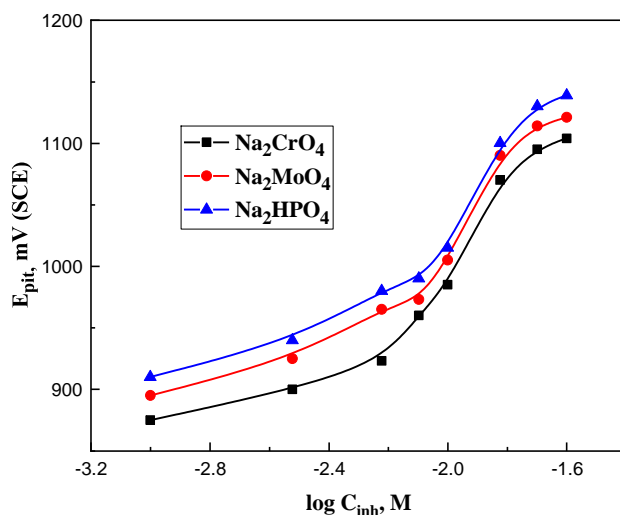


**Figure 8.** Variation of  $E_{pitting}$  with  $\log C_{inh}$  for Ni in 0.01 M  $H_2SO_4$  containing 0.01 M  $Na_2ClO_4$ , at 25°C.

The reliance of the pitting corrosion potential,  $E_{pit}$  of the Ni electrode on the amount of the added inhibitor is depicted in Fig 8. S-shaped curve is obtained with a displacement in the  $E_{pit}$  values into the more positive values (noble direction) with raising the concentration of the inhibitor. Such behavior confirms that the added salt act as an effective inhibitor competing with  $ClO_4^-$  ions to prevent the attack of  $ClO_4^-$  ions by the way of an adsorption mechanism [42].

The existence of the various used anions tolerates the pitting corrosion of Ni in 0.01 M H<sub>2</sub>SO<sub>4</sub> and 0.01 M ClO<sub>4</sub><sup>-</sup> ions following the sequence: phosphate > molybdate > chromate. This trend confirms the increased tendency of the used salts towards pitting corrosion. Molybdate is minimal while HPO<sub>4</sub><sup>2-</sup> is strongly efficacious as pitting corrosion passivators. The inhibition influence of the using salts could be related to the competitive adsorption between the corresponding anion and the ClO<sub>4</sub><sup>-</sup> ions on the passive Ni surface which retards the destructive effect of ClO<sub>4</sub><sup>-</sup> ions by shifting E<sub>pit</sub> into the positive direction preventing pitting corrosion[43]. The adsorbed anions may be combined into the passive film improving the passivity against the destructive effect of ClO<sub>4</sub><sup>-</sup> ions[43].

The inhibition influence of the HPO<sub>4</sub><sup>2-</sup> anions may be owing to the specific passivation of nickel by the precipitation of the nickel-phosphate from the investigated solution, the coagulation on the nickel-phosphate salts on the Ni surface sustains the conditions appropriate for common oxide film [44].

The inhibition effect of MoO<sub>4</sub><sup>2-</sup> ions discussed before by Rafaey et al. [44-46] on the basis of reduction of the Mo<sup>6+</sup> to Mo<sup>4+</sup> that is incorporated in the passive film as a MoO<sub>2</sub> sustaining the healing resistance of oxide film, ( reaction 5):



The reduction of the MoO<sub>4</sub><sup>2-</sup> ions into MoO<sub>2</sub> could furnish supplemental oxygen that impeded the capability of ClO<sub>4</sub><sup>-</sup> and/or Cl<sup>-</sup> ions to adsorb on the Ni electrode surface, preventing the formation of local active cell [42]. Fig 9 depicts the scanning electron micrograph (SEM) of the anodic polarized Ni sample in 0.01 M H<sub>2</sub>SO<sub>4</sub> containing 0.01M ClO<sub>4</sub><sup>-</sup> and 0.01M MoO<sub>4</sub><sup>-</sup> anions. The photograph indicates a less corroded surface with corrosion products spread on the passive metal surface, which confirms the protective effect of the added MoO<sub>4</sub><sup>-</sup> anions.

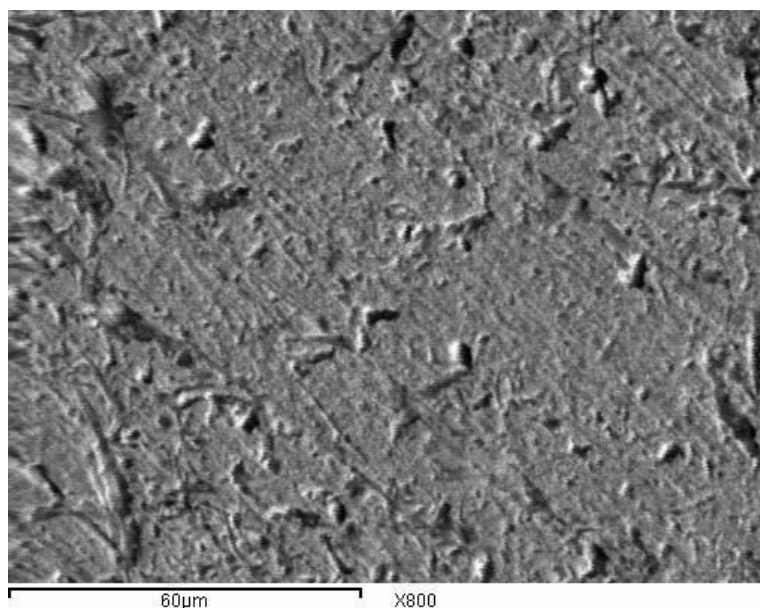


**Figure 9.** Scanning electron micrograph (SEM) of the anodically polarized Ni sample in 0.01 M H<sub>2</sub>SO<sub>4</sub> containing 0.01M ClO<sub>4</sub><sup>-</sup> and 0.01M MoO<sub>4</sub><sup>-</sup> ions.

The inhibition effect of  $\text{Na}_2\text{CrO}_4$  could be interpreted on the basis of the reduction of the hexavalent chromium  $\text{Cr}^{6+}$  to trivalent chromium  $\text{Cr}^{3+}$  to form  $\text{Cr}_2\text{O}_3$  which is easily incorporated into the passive Ni-oxide film in similar to the Fe-passive film [42, 46, 47]. From another point of view, Rafaey et al. [44] attributed the inhibition influence of chromate anions on the pitting of steel is due to the ability of these anions to block the pores spread on the surface of the passive oxide film rising the resistance towards the pitting corrosion.

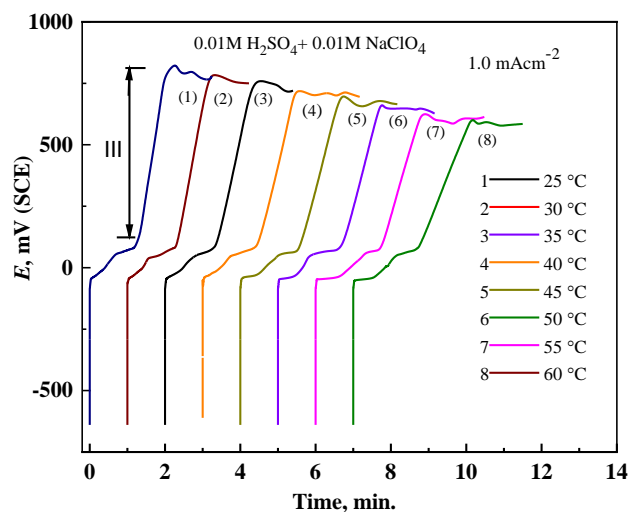


**Figure 10.** The effect of temperature on the anodic polarization curves of Ni in 0.01 M  $\text{H}_2\text{SO}_4$  containing 0.01 M  $\text{NaClO}_4$  solution.

### 3.3. The influence of temperature

The influence of temperature on the anodic polarized curves of Ni in 0.01M  $\text{H}_2\text{SO}_4$  containing 0.01 M  $\text{ClO}_4^-$  ions without and with the additions of 0.01 M of different passivators was investigated. Fig 10 explores the influence of temperature (15-60°C) on the anodic polarized curves of nickel in 0.01 M  $\text{H}_2\text{SO}_4$  containing 0.01 M  $\text{NaClO}_4$  solution. Similar curves are done in presence of 0.10 M  $\text{H}_2\text{SO}_4$  + 0.01 M  $\text{ClO}_4^-$  containing 0.01 M of different inhibitors (curves not shown). It is noted that the raise in the solution temperature increases the induction time needed for the active corrosion and the pitting corrosion. On the another hand, the rate of oxide film formation is decreased with shifting the pitting corrosion potential,  $E_{\text{pit}}$ , (in the absence and presence of the inhibitive anions) into more active values with rising the temperature. The increase in the induction time required for Ni oxidation with the reduction in the rate of building of the Ni oxide film by increasing in the temperature can be explained to the probability of increasing the mobility of ions [48].

The induction period required for the passivation and pitting corrosion processes,  $\tau_1$ , are raised with temperature, while the rate of oxide film formation is reduced through lowering in the slope of the potential-time curve (zone III) of Fig 10. This attitude can be confirmed by Fig 11 which depicts a straight-line relation between the  $\log \tau$  and the temperature, T.

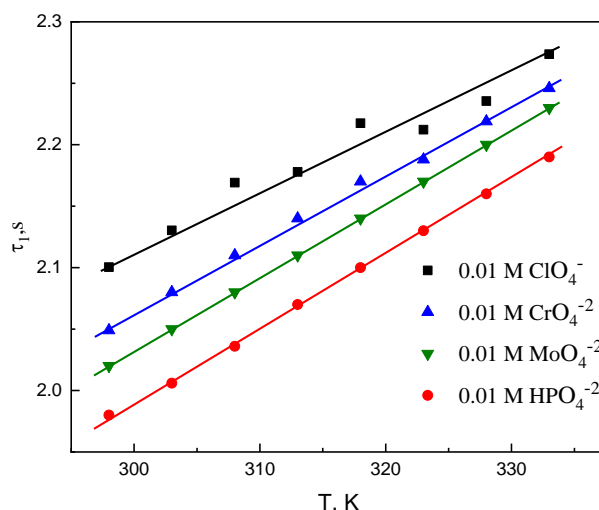


**Figure 11.** Variation of the induction period  $\tau_1$  on the temperature,  $T$ , for Ni in 0.01 M  $\text{H}_2\text{SO}_4$  containing 0.01 M  $\text{NaClO}_4$  solution in the absence and presence of 0.01 M of different anions.

However, the Arrhenius equation [4, 49-58] can be used to calculate the activation energy,  $E_a$ , for damage of the passive oxide film on Ni and initiate the pitting corrosion without and with the used anions.

$$\log r = \frac{-\Delta E_a}{2.303RT} + \log A \tag{11}$$

where  $r$  depicts the rate of corrosion reaction represented by the quantity of electricity ( $Q_a$ ) required to reach  $E_{\text{pit}}$ ,  $E_a$  is the apparent activation energy,  $T$  is the absolute temperature,  $A$  is the Arrhenius constant and  $R$  is the gas constant.

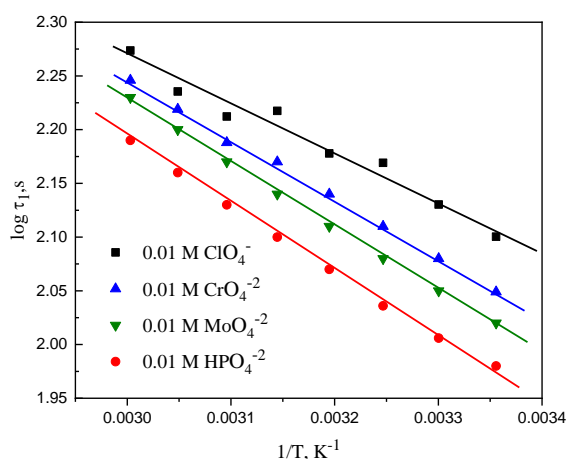


**Figure 12.** Arrhenius plots for Ni in 0.01M  $\text{H}_2\text{SO}_4$  containing 0.01 M  $\text{NaCl}$  and 0.01 M of different inhibitors.

The values of  $\log r$  (in units of  $\text{mC}/\text{cm}^2$ ), calculated at various temperatures are plotted against  $1/T$ , Fig 12, in the case of  $0.01 \text{ M H}_2\text{SO}_4 + 0.01 \text{ M NaClO}_4$  without and with  $0.01 \text{ M}$  of various inhibitors. The activation energies,  $E_a$  were determined from the slope values, Table 1. The activation energy,  $E_a$ , for the pitting corrosion of Ni in  $0.01 \text{ M H}_2\text{SO}_4$  containing  $0.01 \text{ M NaClO}_4$  was  $9.39 \text{ kJ/mol}$ . The existence of the different passivators rise the value of  $E_a$  to be  $11.28$ ,  $12.63$  and  $14.36 \text{ kJ/mol}$  with  $\text{CrO}_4^{2-}$ ,  $\text{MoO}_4^{2-}$  and  $\text{HPO}_4^{2-}$ , successively. The increase in the  $E_a$  values with the used passivators explain the increase in the energy barrier, which is accompanied by the reduction in charge and mass transfer [50].

#### 4. CONCLUSION

The anodic polarization of Ni in dilute  $\text{H}_2\text{SO}_4$  containing  $0.01 \text{ M NaClO}_4$  was examined without and with various additions of  $\text{CrO}_4^{2-}$ ,  $\text{MoO}_4^{2-}$  and  $\text{HPO}_4^{2-}$ . The data indicated that:

- The existence of activation region due to the oxidation accompanied by a linear increase in the potential owing to the oxide film formation followed by  $\text{O}_2$  production.
- Presence of  $\text{ClO}_4^-$  ions destructs the oxide film passivity at  $E_{\text{pit}}$  with initiation of localized pitting corrosion.
- The rate of oxide film formation was reduced with the more additions of  $\text{ClO}_4^-$  ions
- $E_{\text{pit}}$  shifts into less positive values with increasing rising the amount of  $\text{ClO}_4^-$  ions.
- The increase in the induction time with the amount of  $\text{ClO}_4^-$  ions was attributed to the adsorption of the added ions.
- The activation energies required for oxide film destruction and initiation of pitting,  $E_a$ , are increased in the presence of the passivators.

**Table 1.** The activation energy for pitting corrosion,  $E_a$ , of Ni in  $0.01 \text{ M H}_2\text{SO}_4$  containing  $0.01 \text{ M ClO}_4^-$  ions in the absence and presence of different passivators.

Type of anions	$r^2$	$E_a, \text{ kJ mol}^{-1}$
$0.01 \text{ M ClO}_4^-$	0.988	9.39
$0.01 \text{ M ClO}_4^- + 0.01 \text{ M CrO}_4^{2-}$	0.999	11.28
$0.01 \text{ M ClO}_4^- + 0.01 \text{ M MoO}_4^{2-}$	0.998	12.63
$0.01 \text{ M ClO}_4^- + 0.01 \text{ M HPO}_4^{2-}$	0.998	14.34

## References

1. A.I. Muñoz, J.G. Anton, J.L. Guignon, V.P. Herranz, *Corros. Sci.*, 48 (2006) 3349.
2. J.L. Trompette, L. Massot, H. Vergnes, *Corros. Sci.*, 74 (2013) 187.
3. S.M. Abd El-Haleem, S. Abd El-Wanees, *Prot. Met. Phys. Chem.*, 54 (2018) 859.
4. S. Abd El Wanees, M. Abdallah, A.S. Al-Gorair, F.A.A. Tirkistani, S. Nooh, R. Assi, *Int. J. Electrochem. Sci.*, 16 (2021) 150969.
5. M. Abdallah, S. Abd El Wanees, R. Assi, *Port. Electrochim. Acta*, 27 (2009) 77.
6. Y. Xie, T. Dinh, N. Jianqiang, Z. David, J. Young, *Corros. Sci.*, 146 (2019) 28.
7. M. Abdallah, I. A. Zaafarany, S. Abd El Wanees, R. Assi, *Int. J. Electrochem. Sci.*, 9 (2014) 1071.
8. G. Cordeiro, O. R. Mattos, O. E. Barcia, L. Beaunier, C. Deslouis, B. Tribollet, *J. Appl. Electrochem.*, 26 (1996) 1083.
9. E.M. Mabrouk, H.E. Megahed, M. Abdallah, A.A. Abdel Fattah, *Bull. Electrochem.*, 11 (1995) 217.
10. S. M. Abd El-Haleem, S. Abd El-Wanees, *Mater. Chem. Phys.*, 128 (2011) 418.
11. S.C. Britton and U.R. Evans, *J. Chem. Soc.*, (1930) 1773.
12. E. Kunze and K. Schwabe, *Corros. Sci.*, 4 (1964) 109.
13. J.O. Bockris, A.K.N. Reddy, and B. Rao, *J. Electrochem. Soc.*, 113 (1966) 1133.
14. G. Dibari and J.V. Petrocelli, *J. Electrochem. Soc.*, 112 (1965) 99.
15. A. Pigeaud, *J. Electrochem. Soc.*, 122 (1975) 80.
16. A.J. Arvia and D. Posadas, "Nickel" in *The Electrochemistry of the Elements*, Vol. III., A.J. Bard, ed., Marcel Dekker, Inc., New York, NY, 1975, 212.
17. G.S. Frankel, *J. Electrochem. Soc.*, 145 (1998) 2186.
18. P.C. Pistorius, G.T. Burstein, *Philos. Trans. R. Soc. Lond. Ser. A. Math. Phys. Eng. Sci.*, 341 (1992) 531.
19. R.C. Newman, 2001 W.R. Whitney Award Lecture, *Corrosion*, 57(2001) 1030.
20. G.S. Frankel, N. Sridhar, *Materials Today*, 11 (2008) 38.
21. T. Li, J. Wu, G.S. Frankel, *Corros. Sci.*, 182 (2021) 109277.
22. M. Abdallah, I.A. Zaafarany, S. Abd El Wanees, R. Assi, *Int. J. Corros. Scale Inhib.*, 4(2015) 338.
23. M. Pagitsas, M. Pavlidou, D. Sazou, *Electrochim. Acta*, 53 (2008) 4784.
24. D. Sazou, A. Kominia, M. Pagitsas *J. Solid State Electrochem.*, 18 (2014) 347.
25. S. Abd El Wanees, E.E. Abd El Aal, A. Abd El Aal, *Anti-Corros. Meth. Mater.*, 38 (1991) 4.
26. L. Li, S.-H. Chen, X.-G. Yang, C. Wang, W.-J. Guo, *J. Electroanal. Chem.*, 572 (2004) 41.
27. E.E. Foad El-Sherbini, *Corros. Sci.*, 48 (2006) 1093.
28. S. Abd El Wanees, M.I. Alahmdi, M.A. Alsharif, Y. Atef, *Egypt. J. Chem.*, 62 (2019) 811.
29. M.G.A. Saleh, S. Abd El Wanees, S. Khalid Mustafa, *Chem. Eng. Commun.*, 206 (2019) 789.
30. S. Abd El Wanees, S.H. Seda, *J. Disper. Sci. Technol.*, 40 (2019) 1813.
31. S. Abd El Wanees, E. E. Abd El Aal, *Corros. Sci.*, 52 (2010) 338.
32. F. M. Abd El wahab, J. M. Abd El kader, H.A. El Shayed, A.M. Shams El Din, *Corros. Sci.*, 18 (1978) 997.
33. E.E. Abd El Aal and S. Abd El Wanees, *Corros. Sci.*, 51 (2009) 458.
34. B. Mac Dougal, D.F. Mitchell, M.J. Graham, *J. Electrochem. Soc.*, 127 (1980) 1248.
35. M. Pourbaix, *Atlas of Electrochemical Equilibria*, Pergamon Press, Oxford, UK (1996) 330.
36. R. Nishimura, M. Araki, and K. Kudo, *Corrosion NACE*, 43 (1987) 486.
37. E.E. Abd El Aal, *Corros. Sci.*, 45 (2003) 759.
38. F.M. Abd El Wahab, J.M. Abd El Kader, H.A. El Shayeb, A.M. Shams El Din, *Corros. Sci.*, 18 (1978) 997.
39. J. Soltis, *Corros. Sci.*, 57 (2015) 5.
40. E.E. Abd El Aal, *Corros. Sci.* 42 (2000) 1.
41. B. MacDougall, *J. Electrochem. Soc.* 136 (1979) 919.
42. S.M. Abd El Haleem, S. Abd El Wanees, E.E. Abd El Aal, A. Farouk, *Corros. Sci.* 68 (2013) 1.

43. S.M. Abd El Haleem, S. Abd El Wanees, E.E. Abd El Aal, A. Diab, *Corros. Sci.*, 52 (2010) 292.
44. S.A.M. Refaey, S.S. Abd El Rehim, F. Taha, M.B. Saleh, R.A. Ahmed, *Appl. Surf. Sci.*, 158 (2000) 190.
45. S.A.M. Refaey, *Appl. Surf. Sci.*, 240 (2005) 396.
46. Z.H. Dong, X.P. Guo, J.X. Zheng, L.M. Xu, *J. Appl. Electrochem.*, 32 (2002) 395.
47. Y.F. Cheng, B.R. Rairdau, J.L. Luo, *J. Appl. Electrochem.*, 28 (1998) 1371.
48. S.S. Zumdahl, *Chemistry*, 3<sup>rd</sup> Ed, D.C. Heath & Co. (1993) 645.
49. S.M. Abd El Haleem, S. Abd El Wanees, A. Bahgat, *Corros. Sci.*, 87(2014) 321.
50. A. Attou, M. Tourabi, A. Benikdes, O. Benali, H.B. Quici, F. Benhiba, A. Zarrouke, C. Jama, F. Bentiss, *Coll. Surf. A: Physicochem. Eng. Aspects*, 604 (2020) 125320.
51. M. Abdallah, H.M. Altass, A.S Al-Gorair, J. H. Al-Fahemi, K.A. Soliman, *J. Mol. Liq.*, 323 (2021) 115036.
52. M. Abdallah, F. H. Al-abdali, R. El-Sayed, *Chem. Data Collect.*, 28 (2020) 100407.
53. S. Abd El Wanees, A.A. H. Bukhari, N.S. Alatawi, S. Salem, S. Nooh, S.K. Mustafa, S.S. Elyan, *Egypt J. Chem.*, 65(2021) 547-559.
54. S. Abd El Wanees, S.H. Seda, *J. Disper. Sci. Techn.*, 40 (2019) 1813.
55. S. Abd El Wanees, Mohamed I. Alahmdi, M. Abd El Azzem, H.E. Ahmed, *Int. J. Electrochem. Sci.*, 11 (2016) 3448.
56. S. Abd El Wanees, M.I. Alahmdi, S.M. Rashwan, M.M. Kamel, and M.G. Abd Elsadek, *Int. J. Electrochem. Sci.*, 11 (2016) 9265.
57. S. Abd El Wanees, A.B. Radwan, M.A. Alsharif, S.M. Abd El Haleem, *Mater. Chem. Phys.*, 190 (2017) 79.
58. S. Abd El Wanees, A. Diab, O. Azazy, M.A. El Azim, *J. Disper. Sci. Techn.*, 35 (2014) 1571.